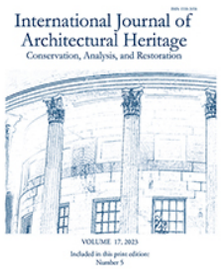

International Journal of Architectural Heritage

Conservation, Analysis, and Restoration

ISSN: (Print) (Online) Journal homepage: https://www.tandfonline.com/loi/uarc20

Titania-silica Composite with Photocatalytic Properties and Its Application on Brazilian Granite and Sandstone

Danielle Grossi, Dolores Ribeiro Ricci Lazar, Eliane Aparecida Del Lama & Valter Ussui

To cite this article: Danielle Grossi, Dolores Ribeiro Ricci Lazar, Eliane Aparecida Del Lama & Valter Ussui (2023) Titania-silica Composite with Photocatalytic Properties and Its Application on Brazilian Granite and Sandstone, International Journal of Architectural Heritage, 17:5, 770-787, DOI: 10.1080/15583058.2021.1969483

To link to this article: https://doi.org/10.1080/15583058.2021.1969483

Published online: 13 Sep 2021.

INTERNATIONAL JOURNAL OF ARCHITECTURAL HERITAGE
2023, VOL. 17, NO. 5, 770–787
https://doi.org/10.1080/15583058.2021.1969483

Titania-silica Composite with Photocatalytic Properties and Its Application on Brazilian Granite and Sandstone

Danielle Grossi [a], Dolores Ribeiro Ricci Lazar [b], Eliane Aparecida Del Lama [a], and Valter Ussui [b]

[a]Mineralogy and Petrology Department, University of São Paulo, São Paulo/SP, Brazil; [b]Instituto de Pesquisas Energéticas e Nucleares, IPEN/CNEN, São Paulo/SP, Brazil

ABSTRACT

The aim of the study described in this article was to evaluate a product containing titania (titanium dioxide, TiO_2) applied on stones — particularly two types used at Brazilian stone-built heritage sites — that have been exposed to weathering and anthropogenic activities. This product was prepared by producing a suspension of TiO_2 at two concentrations (1% and 4% w/v) with tetraethyl orthosilicate (TEOS) in the presence of n-octylamine as surfactant. The characteristics of the TiO_2 were then observed by scanning electron microscopy (SEM), Brunauer-Emmett-Teller (BET) surface-area measurements, particle-size distribution analysis (CILAS) and X-ray diffraction. After applying the TiO_2-TEOS composite, the stones were examined for contact angle, spectrophotometry, sorptivity, thermal shock resistance, and UV-radiation resistance. The product proved ineffective on Itararé sandstone, mainly due to its mineralogical components, as the product does not adhere to quartz. When applied on Itaquera granite, the 1% TiO_2 (w/v) concentration proved to be an appropriate treatment, as it demonstrated better thermal shock resistance, photocatalytic activity, porosity maintenance, and global colour when compared to the 4% concentration.

ARTICLE HISTORY
Received 6 December 2019
Accepted 13 August 2021

KEYWORDS
Architectural heritage; Itaquera granite; Itararé sandstone; photocatalysis; self-cleaning surfaces; stone conservation; Tio_2-Teos composite

1. Introduction

The conservation of heritage-status buildings and monuments located in large cities is a challenge for many countries. Long-term exposure to the effects of weathering and anthropogenic activities, which include pollutant emissions, urine, graffiti, and poor maintenance, contributes to faster surface degradation of the constructions exposed to these elements. To counteract such effects, it is fundamentally important to study new products for protecting stone-built heritage sites. Most of the recent studies with this aim have focused on the effectiveness of the application of products containing titania (TiO_2).

The more traditional use of TiO_2 is as a white pigment in paints, coatings, paper, and plastics (Feltrin et al. 2013; Pinho and Mosquera 2013). The photocatalytic properties of TiO_2 with submicron or nano-scale particle sizes was originally used in both water and air purification. These substances are also capable of removing industrial compounds due to their photocatalytic properties (self-cleaning, depolluting, and antibacterial) — a fact worth noting, as such depolluting characteristics also benefit the surroundings of treated surfaces and make the substances very useful for inhibiting biodeterioration (Pinho and Mosquera 2013).

Some authors have studied the application of TiO_2 due to its biocidal properties (La Russa et al. 2014), self-cleaning (superhydrophilic), photocatalytic characteristics, non-toxicity, chemical stability, and photostability over a broad pH range (Fujishima, Rao, and Tryk 2000; Nogueira and Jardim 1998). Owing to these properties, TiO_2 has been used in environmental purification, deodorisation, sterilisation, and self-cleaning applications (Euvananont et al. 2008).

TiO_2 has three polymorphs: anatase and rutile, belonging to a tetragonal crystal system, and brookite, which has an orthorhombic symmetry. Of the three, the polymorphs most commonly used in stone-building conservation are anatase, rutile, and mixtures of the two in various proportions (Andronic et al. 2011; Pinho and Mosquera 2011, 2013). The rutile polymorph has yellowish acicular particles. Anatase has rounded, bluish-coloured particles and proves to be superior to rutile in terms of its larger surface area (Gherardi, Goidanish, and Toniolo 2018; Goffredo et al. 2017;

CONTACT Danielle Grossi dannigrossi@gmail.com Mineralogy and Petrology Department, University of São Paulo, Rua Do Lago 562, São Paulo/SP, Brazil, 05508-080

Quagliarini et al. 2013), high concentration of active sites, greater electron mobility (Hanaor and Sorrell 2011; Kaleji et al. 2011), high transparency and photocatalytic activity, and slower electronic recombination (Nakajima et al. 2000). However, it has a larger band gap than rutile and is unstable at high temperatures (Feltrin et al. 2013), but this is not relevant to treating the surfaces of monuments, since they do not reach high temperatures even when exposed to intense solar radiation.

In Europe, TiO_2 has been used in the development of coating mortars with self-cleaning characteristics (Flores-Colen, Soares, and Brito 2013; Sikora et al. 2017), inhibition of microalgae growth in clay bricks (Graziani et al. 2013), gypsum plaster repair (Franzoni et al. 2014), and also on stones used for constructions, such as Roman travertine (Fiorentino, Grillini, and Vandini 2015), Noto calcarenite, and Carrara marble (Gherardi et al. 2016). In Brazil, its use is relatively new (Scharnberg et al. 2020; Vieira 2016).

Tetraethyl orthosilicate, also known as TEOS, is one of the most commonly used products for consolidating stone, mainly sandstone and granite. It is resistant to ultraviolet radiation, which makes it ideal for use in outdoor areas (Wheeler 2005). It forms relatively strong silicon-oxygen bonds that have high thermal and oxidative stability, presenting good results on stones with moderate degradation. On very degraded stones, however, this product fails to show a good consolidation capacity (Price 2006). The deposition of silica gel via the application of TEOS causes two simultaneous reactions. The first is hydrolysis of the alkoxy group, which separates the ethanol molecules. This reaction can be accelerated by either acid or alkaline catalysis, used in the preparation of most commercial products. Water is essential to this reaction and the subsequent formation of silica gel. Due to this characteristic, TEOS is not effective in arid climates, because the water may evaporate before the gel forms. The second reaction is the condensation of unstable silanols (-Si-OH) to form an amorphous gel (Snethlage and Sterflinger 2011). A major advantage of TEOS is that the other product formed in the reaction is ethanol, which evaporates completely and causes no damage to the stone. Some types of TEOS have water-repellent properties due to the presence of alkyl groups (including methyl, ethyl, i-butyl, and n-octyl) attached directly to silicon. In general, the alkyl groups, formed by siloxanes of varying degrees of cross-linking and molecular weights, may contain reactive alkoxy groups. Diluents include water and organic solvents, such as alcohol or mineral spirits. When water-based, these products interfere with curing of joints, grouts, pointing, plastic repairs and alkoxysilane-based consolidants. Because of this, a pause time of 8 weeks is recommended between the application of the consolidant and the water repellent. The advantages of using a water-repellent consolidant include reduced maintenance time and cost (Wheeler 2005).

A number of studies have been conducted using a TiO_2-TEOS composite for stone protection (Gherardi, Goidanish, and Toniolo 2018; Hendrix et al. 2019; Hilonga et al. 2010; Munafó, Goffredo, and Quagliarini 2015; Pinho and Mosquera 2013; Zanfir et al. 2018). Following this trend, in the present study, a suspension of TiO_2 was synthesised using TEOS in the presence of n-octylamine, a neutral surfactant that interacts weakly with the bond between hydrogen and the silica precursor and is removed by simple drying in ambient air. Its presence prevents cracks in the TEOS gel, helps with the formation of a more homogeneous suspension (Mosquera et al. 2008), and increases the pore size and hydrophobicity of the gel (Xu et al. 2012). The TiO_2 concentrations tested were 1% and 4% (w/v). Higher concentrations of TiO_2 (e.g., 10% w/v) decrease photocatalytic activity due to decreased porosity and greater difficulty in accessing photoactive sites (Pinho and Mosquera 2013).

This composite was applied on two stones of great historical importance to the city of São Paulo: Itararé sandstone, used in the façade of the Municipal Theatre of São Paulo, and Itaquera granite, used in several buildings in the city's historical centre, such as: Obelisk of the Memory, Shopping Center Light, Santo Antônio Church, Metropolitan Cathedral, the Guinle building, the Law Faculty of the University of São Paulo, the portal of the Consolação Cemetery, and the Monument to Ramos de Azevedo, among others (Del Lama et al. 2015).

While there are no previous tests on Itaquera granite, tests carried out with other products on Itararé sandstone had unsatisfactory results (Grossi and Del Lama 2018). More products are still in the research phase. Thus, this stone was chosen for testing in order to find a protective treatment to aid in the theatre's conservation.

2. Materials and methods

2.1. Stone types

Itararé sandstone is a beige to pale-yellow stone. It is known for its varied granulometry and well-marked stratification (Figure 1A and 1B). In thin sections, it is possible to specify its granulometry, which ranges from fine (0.11–0.36 mm) to coarse (0.18–1.1 mm) sand, its

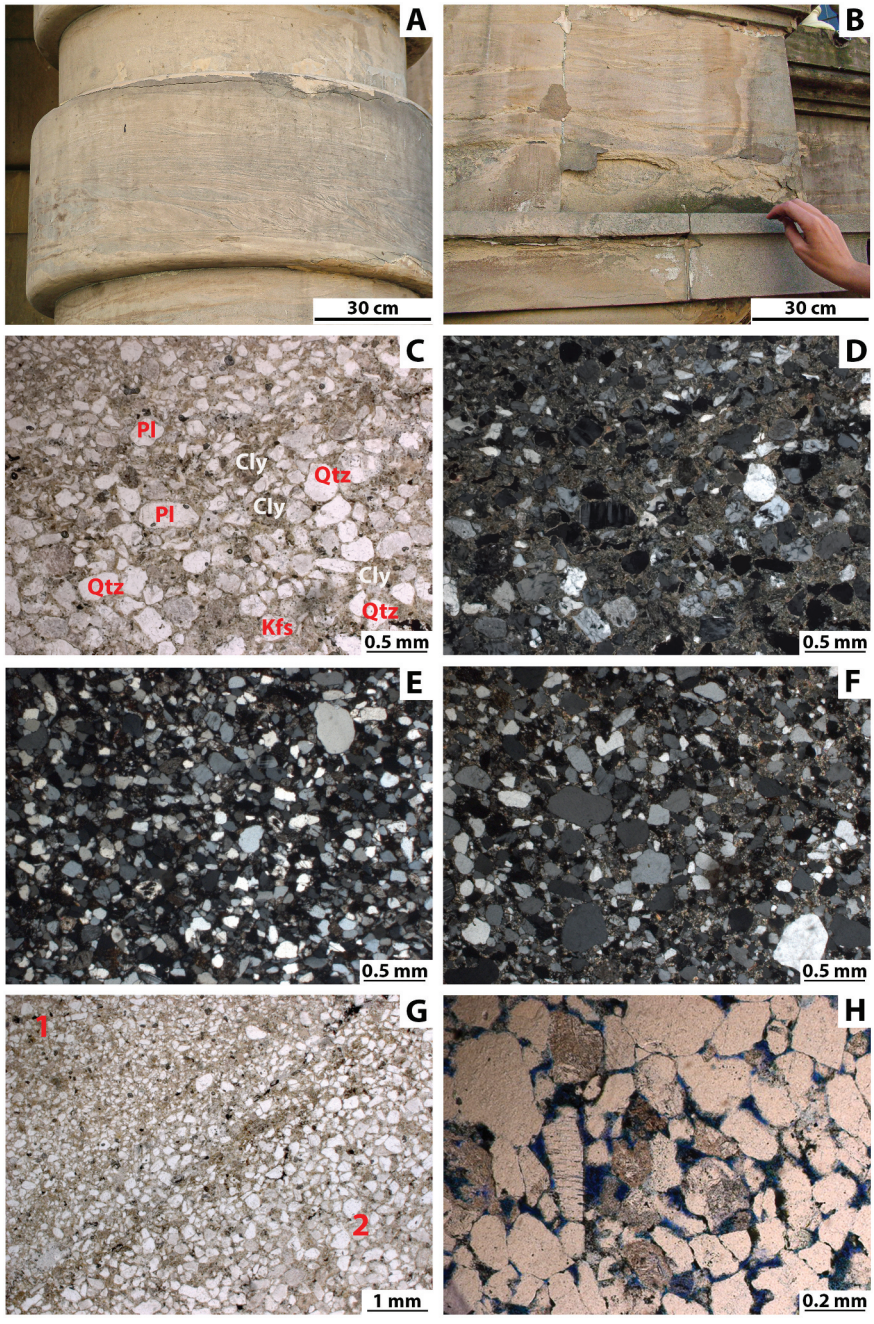

Figure 1. A. Columns of the Municipal Theatre, where it is possible to see the stratification of Itararé sandstone. B. Degradation of Itararé sandstone in the Municipal Theatre caused by swelling clays. C. Petrographic thin section of Itararé sandstone with parallel polarisers. The clay minerals surround the quartz and feldspars grains. D. Same view with crossed polarisers. E. Photomicrograph of finer grains. F. Photomicrograph of coarser grains. G. Itararé sandstone showing stratification and transition from finer (1) to coarser grains (2). H. Porosity stained with blue dye. Qtz = quartz, Pl = plagioclase, Kfs = potassium feldspar, Cly = clay mineral.

grain shape (subrounded to subangular), and its clayey matrix (Figure 1C to 1G) (Del Lama et al. 2008). The minerals found are quartz, plagioclase, potassium feldspar, muscovite, and biotite. Quartz is the main mineral (65–85%), with clear, deformed (exhibiting wavy extinction), or polycrystalline crystals. Feldspars are always present (5–25%), with plagioclase predominating. Its anorthite content and degree of saussuritisation are variable. Potassium feldspar is frequently present, but occurs subordinately. Lithic fragments of volcanic, sedimentary, and metamorphic rocks are present in small quantities. The matrix varies around 10–15% and consists of very fine phyllosilicates. X-ray diffraction analyses have revealed montmorillonite as the fine fraction. Titanite, tourmaline, and zircon have also been observed as accessory minerals. The percentages of minerals were

visually estimated. Pore diameters predominantly ranged from 7.2 μm to 12.9 μm (Del Lama et al. 2008). Porosity ranged from 6% to 13% in the finer-grained strata, and 14% to 18% in the coarser grained strata (Del Lama et al. 2008; Grossi 2016) (Figure 1H).

Itararé sandstone is a problematic stone due to the presence of swelling clays (montmorillonite) (Figure 1B), which greatly accelerate its deterioration (Bocardi et al. 2006; Del Lama et al. 2008; Morenghi 2007).

The use of this stone in buildings includes several slab cuts that differ in their relation to the sedimentary structure, either perpendicular (found in horizontal or vertical positions) or parallel to the stratification.

Itaquera granite has a light grey colour (Figure 2A and 2B), slight foliation, fine crystal size (0.2–2 mm), and very low porosity (0.5%) (Gimenez 2018). It has a low anisotropy due to its only slightly oriented structure (Del Lama et al. 2015; Gimenez 2018). The mineralogy is composed of oligoclase, microcline, quartz, and biotite (Figure 2C and 2D). Oligoclase (38%) occurs as subtabular crystals, many of them zoned, with well-developed saussuritisation and epidotisation processes (Figure 2E and 2F). Microcline (33%) has tartan twinning and some crystals are perthitic. Quartz (18%) shows recrystallisation and strong wavy extinction. Biotite has a green to brownish-green colour and occurs as anhedral aggregates and subtabular crystals. In general, the crystals are corroded. Titanite (1%) and traces of zircon, apatite, and opaque minerals are present as accessory minerals, with epidote (1%) and traces of chlorite, sericite, and carbonate as secondary minerals. Centimetre-scale enclaves of biotite are common (Figure 2B). Its mineral composition indicates

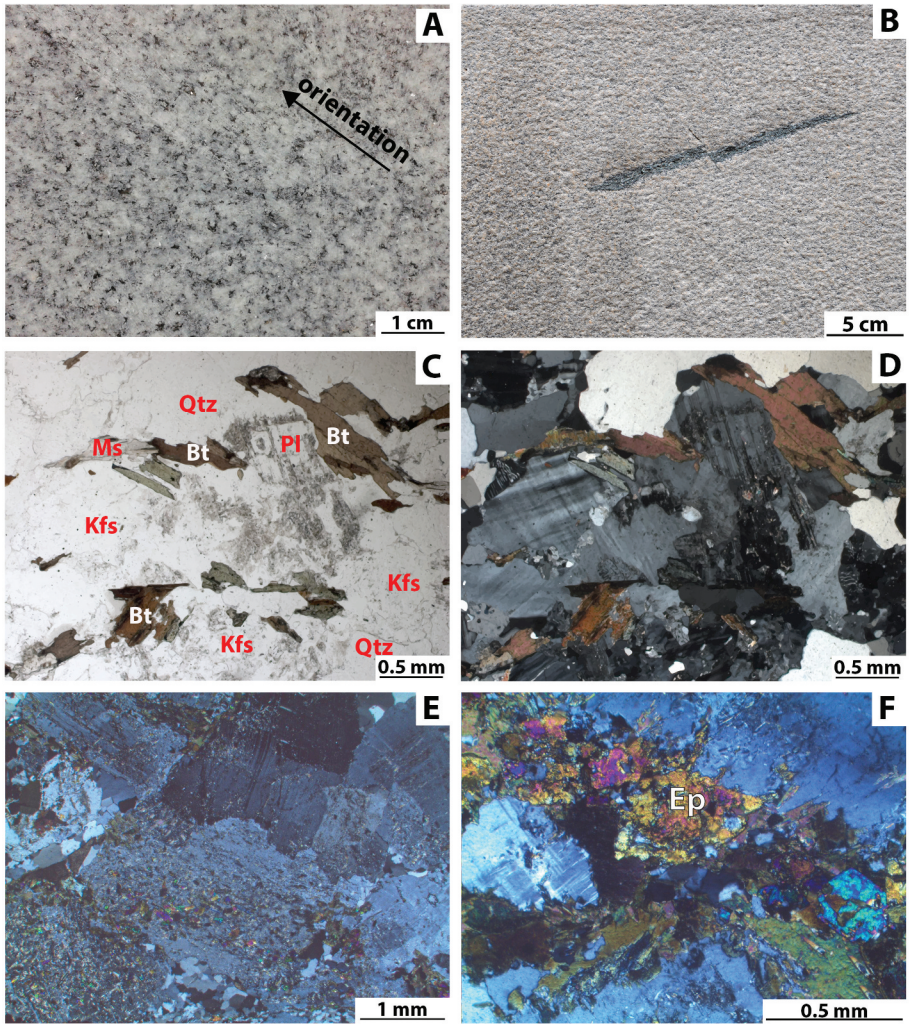

Figure 2. A. Itaquera granite in a hand sample with slight foliation indicated. B. Detail of micaceous enclave with fracture in the middle. C. Petrographic thin section of Itaquera granite with parallel polarisers. D. Same view with crossed polarisers. E and F. Epidote (high-birefringence crystals) formation by hydrothermal alteration. Qtz = quartz, Pl = plagioclase, Kfs = potassium feldspar, Bt = biotite, Ms = muscovite, Ep = epidote.

a hydrothermal alteration because of the wavy extinction and recrystallisation of quartz, curved twin lamellae of plagioclase, curved crystals of biotite, the relative abundance of epidote (Figure 2F), and plagioclase saussuritisation (Del Lama, Dehira, and Reys 2009). It is classified as a biotite monzogranite.

2.2. Synthesis of TiO_2

TiO_2 was laboratory synthesised using the following procedure (Ussui et al. 2003): titanium chloride ($TiCl_3$) was prepared from a commercial TiO_2, resulting in a solution with a TiO_2 content of 47.6 $g.L^{-1}$. Titanium hydroxide was precipitated by adding 100 mL of $TiCl_3$ to 400 mL of 7.5 M ammonium hydroxide solution (NH_4OH) under stirring. The solution coagulated into a gel, which was filtered and washed with water to remove all traces of ammonium chloride (NH_4Cl), followed by washing with ethanol. After filtration, butanol was added to the precipitate prior to solvothermal treatment in an autoclave at 120°C for 4 hours. The remaining butanol was removed by evaporation on a hot plate and in an oven. After this process, the resulting powder was calcined in a muffle furnace at 450°C for 2 hours to form the anatase phase, which has greater photocatalytic activity compared to rutile, mainly due to having particles with a greater surface area (Andronic et al. 2011) and a lower likelihood of electron/gap recombination during photocatalytic action (Hanaor and Sorrell 2011). To reduce the aggregation of the TiO_2 particles, it was then submitted to high-energy grinding in an Atritor mill for 4 hours at a rotational speed of around 200 rpm in an ethanol medium (95% P.A.). The alcohol was removed in an oven at 60°C.

To facilitate the reading of the results, sample abbreviations are listed in Table 1.

Table 1. Sample abbreviations.

Abbreviation	Sample descriptions
UG	Untreated Itaquera granite
G1	Itaquera granite treated with TEOS + 1% (w/v) of TiO_2
G4	Itaquera granite treated with TEOS + 4% (w/v) of TiO_2
GW1	Itaquera granite treated with TEOS + 1% (w/v) of TiO_2 and weathered by thermal shock
GW4	Itaquera granite treated with TEOS + 4% (w/v) of TiO_2 and weathered by thermal shock
US	Untreated Itararé sandstone
S1	Itararé sandstone treated with TEOS + 1% (w/v) of TiO_2
S4	Itararé sandstone treated with TEOS + 4% (w/v) of TiO_2
SW1	Itararé sandstone treated with TEOS + 4% (w/v) of TiO_2 and weathered by thermal shock
SW4	Itararé sandstone treated with TEOS + 4% (w/v) of TiO_2 and weathered by thermal shock

2.3. Composite preparation and application

Once the TiO_2 was synthesized from $TiCl_3$, it was incorporated into a silica matrix to promote adherence to surfaces (Pénard, Gacoin, and Boilot 2007; Pinho and Mosquera 2011). We used this procedure because TiO_2, as a powder, is easily removed from the surfaces on which it is applied (Poulios et al. 1999; Rao, Subrahmanyam, and Boule 2004; Windler et al. 2012). Therefore, the TiO_2 was mixed with TEOS from Sigma Aldrich in the presence of 0.5% by volume of n-octylamine as surfactant (Mosquera et al. 2008). The TiO_2 concentrations used were 1% and 4% (w/v) (Goffredo et al. 2017; Graziani, Quagliarini, and D'Orazio 2016).

The composite was applied in two coats, with a ten-minute interval between applications, using a soft bristle brush on only one face of eighty-six samples of the two types of stone. The samples had dimensions of 8.5 × 2.5 × 1.0 cm, except for those used in the sorptivity test, for which 1 × 1 × 1 cm-sized samples were used. The number of applications was chosen to provide the highest possible deposition of titania with the least colorimetric change. After the composite was applied, the samples were left to dry for two weeks at room temperature. The colour, hydrophobicity, and capillarity of the surfaces were measured before and after treatment and at the end of the weathering tests.

Stone anisotropy is very important when considering the application of conservation treatments (Fort et al. 2011; Sena da Fonseca et al. 2017). The treatment was applied parallel to the stratification of the Itararé sandstone. In the case of granites in general, the orientation and distribution of exfoliation microcracks influence the decay in the different splitting planes (Freire-Lista and Fort 2017). Exfoliation microcracks were not observed in Itaquera granite in the samples we studied, and despite its lightly oriented structure, it can be considered an isotropic stone. For this reason, the position of the stone in the quarry was not considered in the sample preparation.

2.4. Tests

The first tests were done to characterise the TiO_2 synthesis. After that, we characterised the stones before and after the application of the composite.

2.4.1. Tests on the synthetic TiO_2

TiO_2 was characterised by X-ray diffraction (XRD), scanning electron microscopy (SEM), surface area measurements (BET), and particle-size distribution analysis (CILAS).

XRD: The diffractometer was a Rigaku, Multiflex model, using a tube with Kα radiation from Cu (copper). We performed the analysis using the ICDD (International Centre for Diffraction Data) table 21–1272 to check whether the anatase phase was formed.

SEM: The SEM device used was a Quanta FEG 600-FEI, equipped with a Quantax-Bruker EDS microanalysis system (Detector 4030) and a silicon drift detector. For the higher magnification images, a SEM-FEG (JEOL-JSM 6710 F) was used. We used SEM to verify particle shape and size.

BET: For the BET surface area, an ASAP 2010 device from Micromeritics was used. This technique was used to verify the surface area of the particles formed.

CILAS: For the granulometric distribution analysis and to determine the particle/agglomerate size distribution, a CILAS model 1064 was used, operating with an 820-nm laser. The distribution was determined using the Mie method, which is appropriate for particles smaller than 50 μm (Pohl 1998).

2.4.2. Tests on the stones

The tests performed for characterisation of the stones before and after the application of the TiO_2-TEOS composite were: sorptivity, contact angle, spectrophotometry, thermal shock resistance, and UV radiation resistance. Petrography was performed only before the composite application. The application of the composite was only on the surface of the stone and did not change the stone internally, so petrography was not performed after treatment. XRD was also performed to determine the clayey matrix of the Itararé sandstone.

XRD: A Bruker D8 Advance diffractometer with copper tube (Cu Kα) and nickel filter was used. The analyses were performed using the DIFRAC.EVA 4.1 program. The stones were ground and only the clay fraction was separated to be tested by the powder method. With the peak of 14 Å found, the clay fraction was glycolated.

Sorptivity: For the sorptivity test, the bases of sixteen samples of dimensions 1 × 1 × 1 cm were placed in contact with deionised water (immersed by approximately 1–2 mm), and their weights were taken at 0, 5, 10, 15, 20, 30, 60, 120 and 180 minutes.

Contact-angle test: To measure the hydrophobicity of the stone surface, a digital camera equipped with an AF-S Micro NIKKOR 60 mm 1: 2.8 G ED macro lens was positioned 15 cm from the sample, and the photo was taken three seconds after the deposition of one 0.025 mL drop of deionised water. Three drops were deposited on the largest side of two separate samples of each stone/treatment. This test was performed on untreated and treated samples measuring 8.5 × 2.5 × 1.0 cm, which were weathered by thermal shock.

Spectrophotometry: For the spectrophotometry test, a Konica Minolta CM-2500d was used with the following parameters: illuminant D65, specular component included (SCI) and excluded (SCE), observer at an angle of 10° and aperture of 8 mm on samples of 8.5 × 2.5 × 1.0 cm. We performed 225 measurements on forty-seven samples. This test was performed on untreated and treated samples, before and after the thermal shock test and before and during the UV resistance test. The data are presented in accordance with the CIELab (International Commission on Illumination) system. The **L*** parameter indicates changes in luminosity, where 0 = black/dark and 100 = white/light; **a*** has positive values for red and negative values for green; while **b*** has negative values for blue and positive values for yellow; ΔE* refers to the overall colour change. This parameter was calculated using Eq. (1), with the On Color software version 5.4.5.1 being used for data analysis.

$$\Delta E^* = \sqrt{(\Delta L^*)^2 + (\Delta a^*)^2 + (\Delta b^*)^2} \quad (1)$$

Thermal shock resistance: The test for weathering by thermal shock was adapted from ABNT NBR ISO 10545–9/2017. Samples were put in the oven at 100°C for 20 minutes, then placed in running water until cool, and subsequently placed in a vessel filled with water at 17°C for 15 minutes. This procedure was repeated ten times to evaluate resistance to weathering from temperature change. We performed 8 contact-angle measurements per sample on two samples for each treatment, totalling 32 measurements for each type of stone, 64 of these being before the test and another 64 after the test, totalling 128 measurements on samples of 8.5 × 2.5 × 1.0 cm. Only fresh granite was measured because fresh sandstone absorbed each drop of water before it could be photographed. The colour changes were also evaluated in 18 measurements for each stone type, totalling 36 measurements.

UV-radiation resistance: The UV-light resistance test is used to test the self-cleaning property of TiO_2 nanoparticles that discolour an artificial dye, such as rhodamine B, when exposed to UV light. Therefore, TiO_2-treated samples were expected to show greater dye discoloration than untreated samples when exposed to UV light. A 0.05 $g.L^{-1}$ rhodamine B solution was prepared for this test in accordance with (Ruot et al. 2009) to check if the treated sample would discolour. Each sample received 0.5 mL of this solution. After drying for 24 hours in a light-free environment, the samples were positioned 20 cm away from an OSRAM Ultra-Vitalux 300 W lamp, which is a mercury-discharge lamp with a tungsten filament that emits UVA radiation between

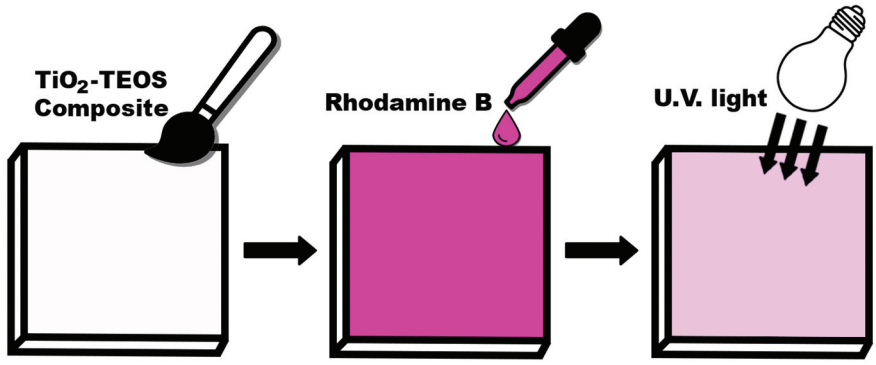

Figure 3. Scheme of UV-light resistance test.

315 and 400 nm and UVB between 280 and 315 nm, radiation similar to that of sunlight (Figure 3). Colour measurements were performed at 0, 15, 30, 60, and 120 minutes. We tested one untreated sample, three samples of both Itararé sandstone and Itaquera granite treated with the TiO_2-TEOS composite with 1% (w/v) TiO_2 content, and three samples of each stone with the composite with 4% (w/v) TiO_2 content. All samples measured 8.5 × 2.5 × 1.0 cm.

3. Results and discussion

3.1. Coating characterisation

The TiO_2 formed anatase with an aggregation of spheroidal crystallites (Figure 4), which is a typical morphology of the synthesis method (Sun et al. 2009; Ussui et al. 2003) due to pH precipitation control (Sun et al. 2009). This morphology is one of several that can be produced by the synthesis of TiO_2. Each of the morphologies has a specific functionality. Spheroidal crystallites, much like nanoflowers and nanotubes, have photocatalytic activity (Reghunath, Pinheiro, and Devi 2021).

The diameter of the agglomerate was 27.23 μm with small crystals of 0.91 μm (Table 2, Figure 5). The particles' diameter was larger than those found in other studies (Quagliarini et al. 2013; Ruot et al. 2009), but in those cases, different chemical raw materials were used.

The surface area of the synthesised TiO_2 was 126.6 $m^2.g^{-1}$, which is close to the highest values mentioned in the literature (Feltrin et al. 2013) regarding TiO_2 synthesised in a laboratory by a hydrothermal process at 200°C. This value is considered high, and the larger the surface area, the better the performance of the product due to the availability of active sites for the photocatalytic reaction. Anatase usually has a larger surface area, and is obtained at a lower calcining temperature, compared to rutile. Therefore, the improved surface properties of anatase can outweigh the benefits of the lower band gap of rutile. Addittionally, anatase has a lower recombination rate between the electron and the hole (Bak et al. 2015; Shtyka et al. 2021). A larger surface area (202–340 $m^2.g^{-1}$) was found in another study (Hilonga et al. 2010). In that case, the authors prepared the TiO_2-TEOS composite from sodium silicate and titanium oxychloride. This value was

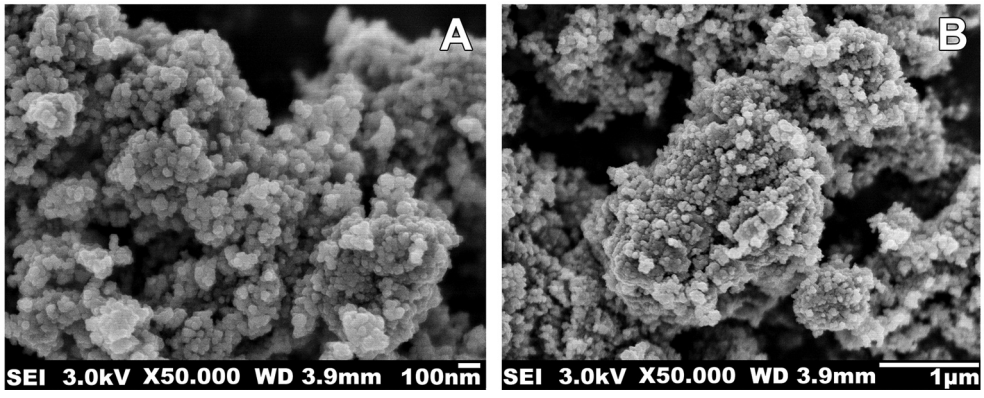

Figure 4. Agglomerated TiO_2 particles observed by SEM-FEG.

Table 2. Analysis of the granulometric distribution of TiO_2.

Employed model	Diameter (μm)	Mean (μm)
Mie	D10: 0.91 D50: 16.40 D90: 71.03	27.23

obtained because silica is an inhibitor of rutile-phase formation and the growth of crystal grains during heat treatment (Hilonga et al. 2010).

3.2. Stone characterisation

The XRD of the clay fraction of Itararé sandstone was performed to verify to which group the clays belong (Figure 6). It was observed that the peak corresponding to the clays (14 Å) was present in the sample. The same sample was subsequently glycolated and a peak of 16 Å was detected. The glycosylation process increases the interplanar distance between clay layers, simulating clay hydration. Therefore, the clays present in Itararé sandstone belong to the group of montmorillonites 2:1, which are expansive clays (Neves 1968).

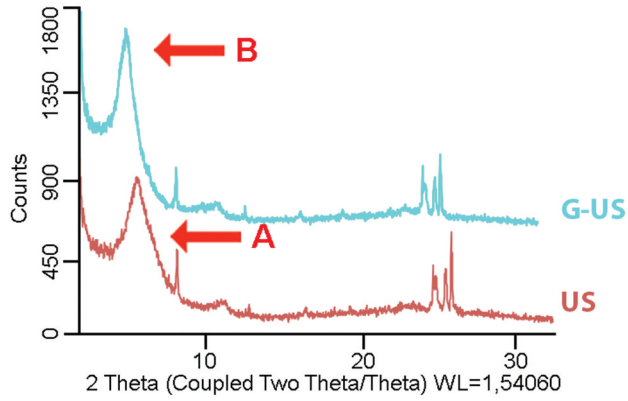

Figure 6. X-ray diffraction of the clay fraction of Itararé sandstone (red line) showing (A) the clay peak (14 Å), and the same sample after glycosylation (turquoise line) showing (B) the swelling-clay peak of the montmorillonites group (16 Å).

3.3. Surface characterisation

The SEM observation of Itararé sandstone treated with 1% TiO_2 (w/v) (S1) (Figure 7A) showed 80% less coverage when compared to the sample treated with 4% TiO_2 (w/v) in TEOS (S4) (Figure 7B). The TiO_2 adhered to the clay matrix, including montmorillonite, but not to quartz and feldspar grains (Figure 7C). This may be due to the smooth surface of these minerals, which hinders adherence by the TiO_2, or to a repulsion of electronic charges between them, given that TEOS is known to be effective with regard to application on quartz stones, as both have a similar chemical composition (silica) (Wheeler 2005) and have been reported by the literature to increase the adhesion of the TiO_2 particles (Pinho and Mosquera 2013). Figure 7D shows in detail the shape of the deposited TiO_2-TEOS particles. Considering that the composition of the stone is rich in

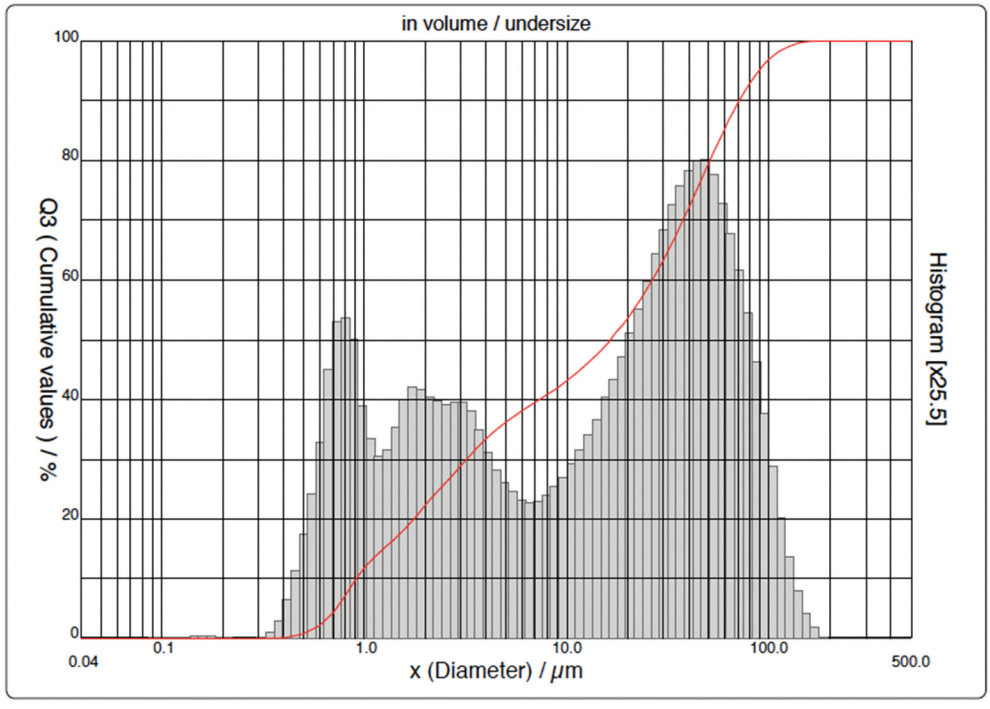

Figure 5. Distribution curve of the agglomerate sizes of synthesised TiO_2.

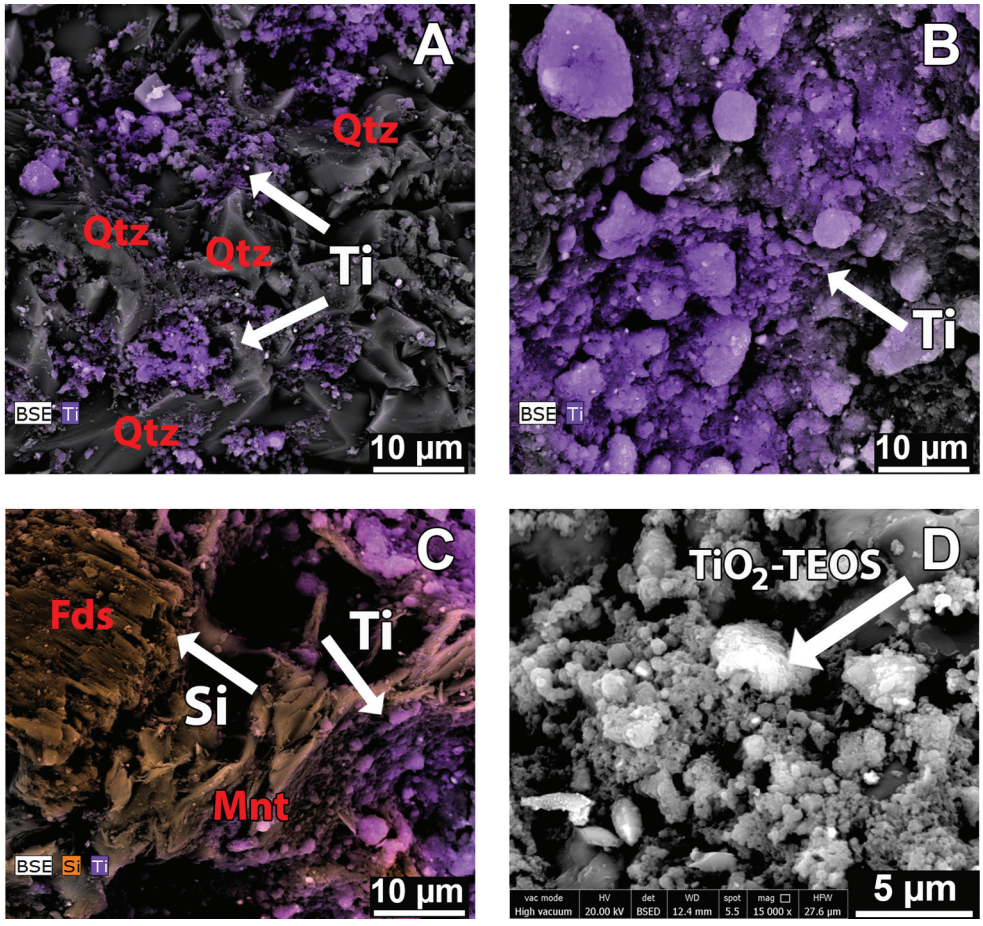

Figure 7. Sample of Itararé sandstone coated with the TiO_2–TEOS composite viewed by SEM: (A) Sample S1 Ti mapping, represented by the colour purple, (B) Sample S4 Ti mapping, represented by the colour purple, (C) Sample S4 Ti and Si mapping, represented by the colours purple and orange, respectively, (D) detail of particles of TiO_2–TEOS deposited on sample S1. Qtz = quartz, Fds = feldspar, Mnt = montmorillonite, Ti = titanium, Si = silicon.

silica, it is difficult to separate the silica content intrinsic to the stone from that contained in the composite powder.

Itaquera granite showed the same behaviour as Itararé sandstone: the samples treated with 1% TiO_2 (w/v) in TEOS (G1) (Figure 8A) displayed less coverage of TiO_2 than those treated with 4% (G4) (Figure 8B), and no TiO_2 was observed in the sites with the highest silica concentration, formed by quartz and feldspar crystals (Figure 8C). In this case, silica was mapped because the underlying stone is not predominantly formed by quartz crystals, as is the case with sandstone. Figure 8D shows the appearance of the particles formed.

In both stones, the deposition of the TiO_2-TEOS composite occurred in the portions richest in phyllosilicates.

Even though cracks are typical in the application of TEOS (Wheeler 2005), no cracks were observed in this study due to the presence of the n-octylamine surfactant (Pinho and Mosquera 2013).

3.4. Water capillarity

Samples S1 and S4 (top of Figure 9) showed sorptivity slightly higher than that observed in the untreated sample, proving that the composite practically does not change in this property. It is worth noting that this stone has granulometric variation, which may be the cause of the scatter observed in the results (Pinho and Mosquera 2013). This fact can be verified by observing the average amount of absorbed water, which was 1161 $g.m^{-2}$ for the untreated sample, 1182 $g.m^{-2}$ for S1, and 1170 $g.m^{-2}$ for S4, representing increases of 2% and 1%, respectively.

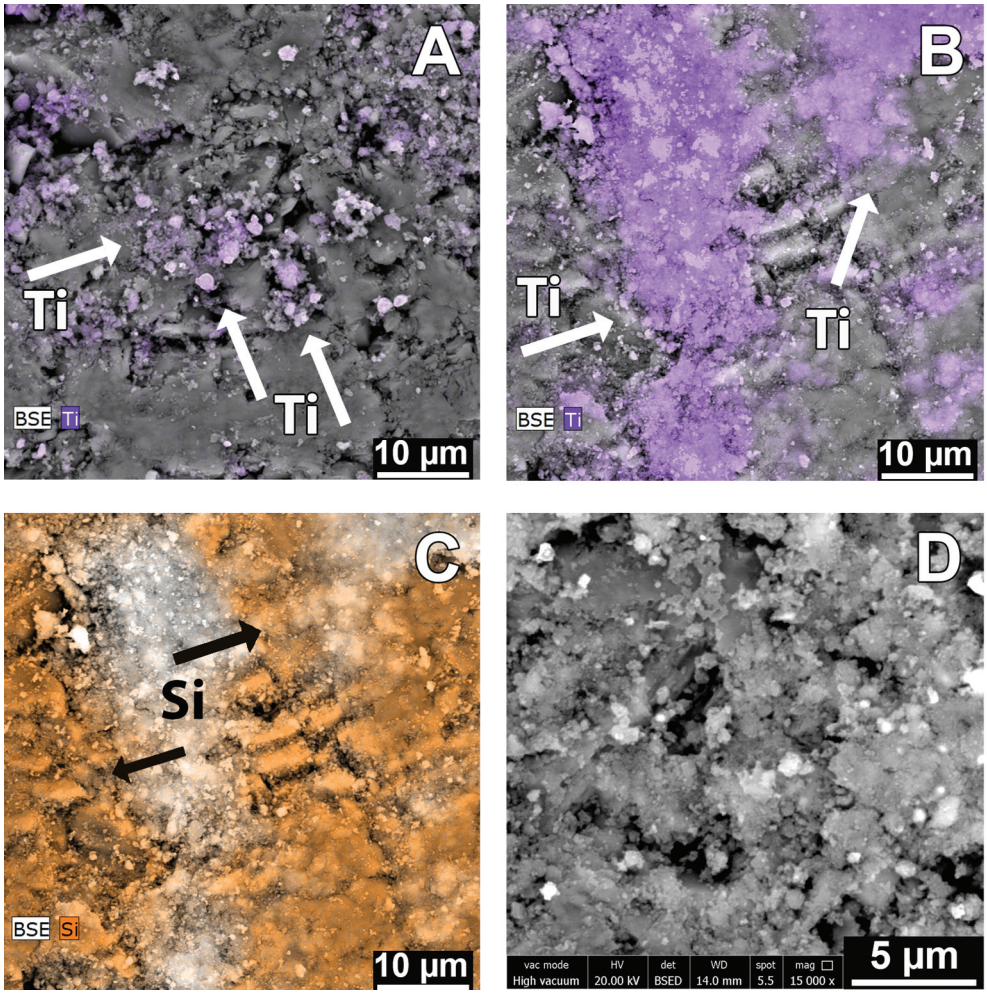

Figure 8. Sample of Itaquera granite treated with TiO_2–TEOS composite viewed by SEM. As the mineral is covered by the composite, it is not possible to observe it. (A) Sample G1 Ti mapping, represented by the colour purple, (B) Sample G4 Ti mapping, represented by the colour purple, (C) G4 sample Si mapping, represented by the colour orange, (D) appearance of the particles formed in sample G4. Ti = titanium, Si = silicon.

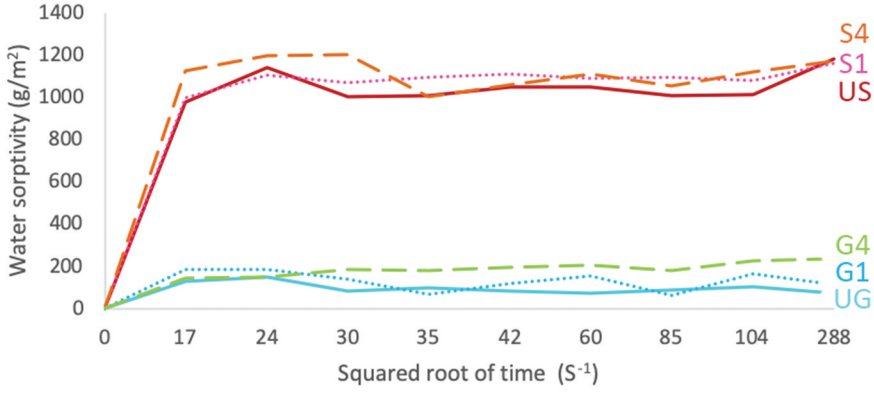

Figure 9. Water sorptivity of the samples studied as a function of time. Itararé sandstone before (US) and after the application of the TiO_2–TEOS composite (S1 and S4). Itaquera granite before (UG) and after the application of the TiO_2–TEOS composite (G1 and G4).

The water-sorptivity graph for Itaquera granite (bottom of Figure 9) shows that there was an increase in the amount of water absorbed between the treated (G1 and G4) and untreated samples, showing that the treatment does not seal the pores of the stone. This fact can be verified by observing the average amount of absorbed water, which was 75 $g.m^{-2}$ for the untreated sample, 115 $g.m^{-2}$ for the G1 samples and 234 $g.m^{-2}$ for the G4 samples. This represents increases of 53% and 212%, respectively. The increase in absorbed water may be due to the hydrophilic character of TiO_2 or the increase in surface area due to its presence. In this case, n-octylamine failed to reduce the surface tension of the initial sol gel. An increase in capillarity of samples treated with TiO_2 was also found in another study (Quagliarini et al. 2013), but in limestone. The increased capillarity found for the Itaquera granite is the only disadvantage of applying the product on it. More studies are being carried out with this composite to develop a hydrophobic product.

3.5. Contact angle and thermal shock resistance

It was not possible to measure the contact angle in the US sample, as no water drops formed because of the hydrophilic character of the stone, which is in turn due to its high porosity (6–18%) (Grossi 2016), mineralogy (basically quartz with a clayey matrix), grain size, stratified structure, and sawn surface, which caused the water to be fully absorbed before a drop could be photographed. After applying the composite, the contact angles were 46° for S1 samples and 21° for the S4 samples, increases of 46% and 21%, respectively (Figure 10). Contact angles between 0° and 90° represent a hydrophilic product (Quagliarini et al. 2012). In this case, S1 showed less hydrophilic behaviour than S4. These contact angles are much smaller than those found in the literature for the use of TEOS and n-octylamine with a commercial TiO_2 (15% anatase and 85% rutile) (Pinho and Mosquera 2013), probably due to the different composition and morphology of the TiO_2 (Reghunath, Pinheiro, and Devi 2021).

After the thermal shock test, the SW1 and SW4 samples returned to the condition observed in the US sample; that is, they absorbed all the water, and no drops formed. This characteristic is considered superhydrophilicity, because the contact angle is smaller than 10° (Banerjee, Dionysiou, and Pillai 2015), showing that, regardless of concentration, as indicated by the contact-angle/wettability parameter, this treatment is not durable for this stone. Thus, after the application of the composite, the stone surface changed from superhydrophilic to hydrophilic. However, after the thermal shock test, the surface went back to displaying a superhydrophilic behaviour, showing that the composite does not have good adhesion resistance when used on this stone, mainly due to its mineralogical composition, which is basically quartz, and thus the composite lost adhesion to the substrate upon the heating of the sample. The high porosity and the grain size also influence the loss of the product's effectiveness after artificial weathering.

The UG samples showed an average contact angle of 4°, which reflects their characteristics, such as low porosity (0.5%), an absence of pores and a matrix with interwoven or juxtaposed crystal contacts. The treated samples showed contact angles of 50° in the case of the G1 samples and 46° for the G4 samples, increases of 1150% and 1050%, respectively. However, only the GW1 samples, which showed a contact angle of 44°, were

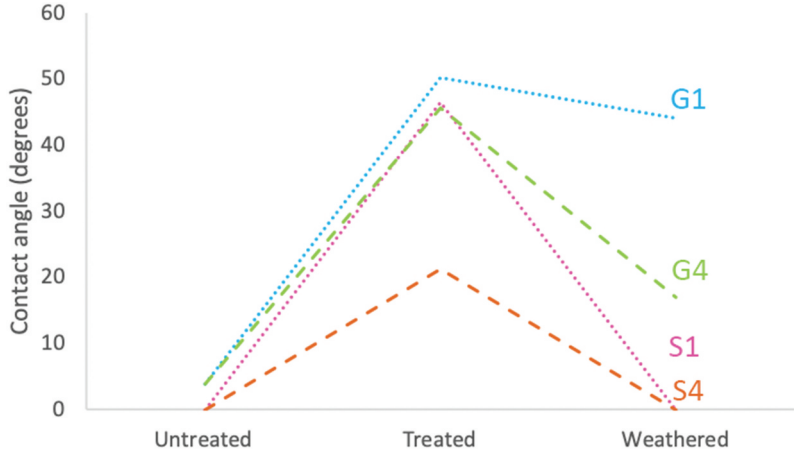

Figure 10. Contact angle of the Itararé sandstone (S1 and S4) and Itaquera granite (G1 and G4) samples: untreated, treated with the TiO_2–TEOS composite, and weathered by thermal shock.

resistant to the thermal shock test. The GW4 samples showed a very small contact angle (17°) after the thermal shock test, indicating that they are less resistant to thermal shock, but have a larger contact angle than that of the untreated stone. The same trend was also observed in marble when a mixture of TEOS and titanium tetra-isopropoxide (TTIP) was used, which showed an increase of 34% in the contact angle (Kapridaki and Maravelaki-Kalaitzaki 2013). Using an aqueous solution of TiO_2, starting with tetrapropylorthotitanate (TPOT) on travertine, an increase of 32% in the contact angle was found (Quagliarini et al. 2013).

Results show that the hydrophilic characteristic of TiO_2 can be observed on both stones. The greater the concentration of the product, the smaller the contact angle. This trend was also found in the literature (Pinho and Mosquera 2013). It could also be observed that — provided the product is the same — the lower the stone's porosity, the wider the contact angle, thus corroborating the results found in the literature (Carrascosa, Facio, and Mosquera 2016). The surface roughness also influences the contact angle. The rougher the surface, the smaller the contact angle (Gherardi, Goidanish, and Toniolo 2018). The product was expected to be hydrophobic, according to one of the articles consulted for this study (Pinho and Mosquera 2013). However, there are differences between the products used, as the silica source used in the work cited contained 41% SiO_2, whereas the source used in the present study had 29% SiO_2. Although silica is hydrophilic, the hypothesis that the difference in concentration could be the reason for the different results was put forward. To test this hypothesis, silica and silicic acid were synthesised in the laboratory to obtain a higher concentration (62.5%). However, this new composite proved to be superhydrophilic, showing that the higher concentration of silica did not make the composite hydrophobic. Nevertheless, commercial products are known to use mixtures in their formulations that are not disclosed and are protected by patent law. The content of such a mixture could be the reason for the hydrophobicity encountered in the work cited.

3.6. Colour changes and photoactivity

Colour changes are affected by the colour of the stone, its finish (sawn, polished, honed, etc.), and the colour of the treatment, in this case TEOS and TiO_2.

When comparing the colorimetric data of untreated and treated Itararé sandstone (Figure 11), it was observed that the S1 samples showed a smaller change in colour, whereas the S4 samples showed a greater chromatic change, mainly in the form of whitening of the surface. Observing the L* parameter, after treatment, S1 showed little change in luminosity, while S4 had a much whiter surface. After thermal shock, S1 became whiter and S4 showed a little reduction in L* values. At the end, the two concentrations of TiO_2 showed similar values: L* = 70.4 for S1 and 72.1 for S4, values higher than those found in the untreated sample. As for the a* parameter after treatment, both concentrations of TiO_2 showed a reduction in the red hue, evidenced by the decrease in positive a* values. After the thermal shock test, S1 continued to show a reduction, while S4 showed

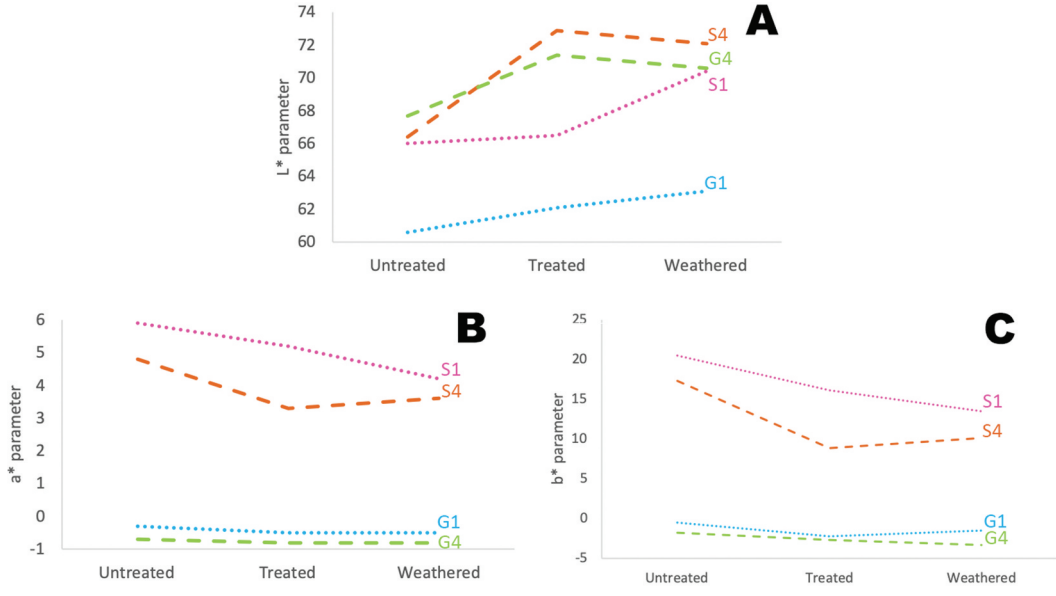

Figure 11. Colorimetric parameters L* (A), a* (B) and b* (C) of the Itararé sandstone and Itaquera granite samples: untreated, treated, and weathered by thermal shock.

a slight increase. Regarding the b* parameter, both samples showed the same trend present in a*, but with a more significant change in values. The colour variation can be confirmed by the ΔE* calculation, which showed a total colour change of 3.9 for the S1 samples and 11.1 for the S4 samples. After the thermal shock treatment, the ΔE* of the SW1 samples increased to 4.8, and the ΔE* of the SW4 samples decreased to 1.5, showing that the 1% concentration of TiO_2 is more resistant to thermal shock.

When comparing the results obtained in the untreated and treated Itaquera granite samples, there was little colorimetric change (Figure 11). The parameter that most altered was L*, with an increase in values and, therefore, a whiter surface due to the coloration of the TiO_2 powder, which is white. After thermal shock, there was an increase in the L* parameter for G1 and a little reduction for G4. The a* parameter did not change with the application of the product nor after the thermal shock, showing that there is no variation in the green/red hues. The b* parameter showed an increase in the blue hue after product application because of the increase in negative values of b*. After thermal shock, G1 showed a reduction and G4 showed an increase in the blue hue. A global assessment of the colorimetric change was performed by calculating the ΔE* after the treatment. G1 showed values of 1.0 and G4 showed 5.1. After thermal shock the ΔE* showed a very small variation: 1.2 for GW1 and 1.0 for GW4, showing that the 1% concentration of TiO_2 is more resistant to thermal shock.

It is worth noting that, while the chromatic change can be detected by the naked eye when ΔE*>3 (Berns 2000), a ΔE* value of ≤5 is considered acceptable in the restoration field (Sasse and Snethlage 1996). However, there is no consensus regarding a ΔE* limit in the literature, as some authors assert that values higher than 4, 5, or 10 (De Ferri et al. 2013; Maravelaki-Kalaitzaki et al. 2008; Ortiz et al. 2013; Toreno et al. 2018) constitute the threshold of human perception. Based on our experiments, we believe that chromatic differences of ΔE*>3 are noticeable to the human eye. As for the samples assessed in the present study, we found that the chromatic change of Itaquera granite was smaller than that of Itararé sandstone. All ΔE* values are shown in Table 3.

Considering ΔE*≤5, only the S4 samples did not demonstrate acceptable colorimetric results. After the thermal shock test, the colours of all samples fell within the acceptable parameters for restoration.

The values found here are similar to the data in the literature. Applying SiO_2 nanoparticles mixed with fluorinated polylactide on marble, ΔE* ranges from 2.2 to 2.4 (Pedna et al. 2016). Another study using M-doped TiO_2 compound on marble showed a ΔE* ranging from 3 to 8. The highest value was found for Fe-doped TiO_2 (La Russa et al. 2012). Using different titania-silica composites (Pinho and Mosquera 2011), ΔE* was found to range from 7 to 15. It should be noted that the chromatic parameters of stones with lighter colours tend to change less. In the case of the stones studied here, Itaquera granite is lighter than Itararé sandstone.

Table 3. Results of performed tests on Itararé sandstone and Itaquera granite.

	Sorptivity (g.m^{-2})	Variation (%)	Contact angle (°)	Contact angle after thermal shock (°)	Variation (%)	ΔE	ΔE after thermal shock	Variation (%)
US	1161	-	-[a]	-[a]	-	-	-	-
S1	1182	+2	46	-[a]	−100	3.9	4.8	+23
S4	1170	+1	21	-[a]	−100	11.1	1.5	−86
UG	75	-	4	-[a]	-	-	-	-
G1	115	+53	50	44	−12	1.0	1.2	+20
G4	234	+212	46	17	−63	5.1	1.0	−80

–[a] — no measurable results.

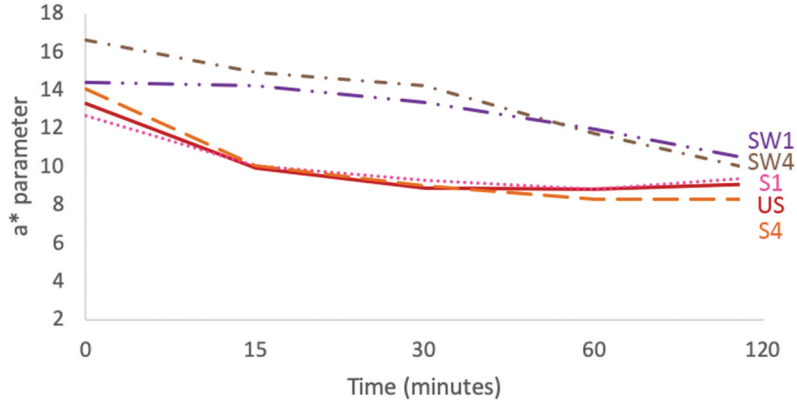

Figure 12. Colour resistance of Itararé sandstone to UV light after application of rhodamine B.

Regarding Itararé sandstone, Figure 12 reveals that S1 samples showed UV-light resistance close to that of the US samples, which is indicated by the discoloration of the dye. S4 samples showed a little larger discoloration of the dye. This shows that the absence of adherence by the product to quartz and the high porosity of the stone made TiO_2 ineffective. After the thermal shock test, the photocatalysis was initially slower, but after a while reached the same values as for untreated and treated samples. The SW4 samples showed a greater concentration of rhodamine B at the beginning of the test, with a high value of a*, but significant dye discoloration after 30 minutes. In this test, the treated samples should show faster and more pronounced discoloration than the untreated sample to denote the photocatalytic activity of TiO_2. This occurred only in the SW4 samples, and it was accentuated after the thermal shock. This shows that although the photocatalytic activity of the composite on the sandstone surface was below expectations, it was resistant to thermal shock. This fact may be explained by the stone's high porosity, which hinders/prevents UV rays from accessing the pores' interiors, preventing activation of the self-cleaning property of the TiO_2 that was deposited in these places and thus making the treatment less effective on high porosity stones. Another possibility is the absence of TiO_2 on quartz (observed using SEM), which is the main mineral in this stone. This shows that higher concentrations of TiO_2 exhibit larger aggregates and are better in terms of self-cleaning. The limiting factor of using high concentrations of TiO_2 for the conservation of historic stone surfaces are the colorimetric change that whitens the surface, the increase in hydrophobicity, and the absence of adhesion to the surfaces.

The G1 and G4 samples showed higher photocatalytic activity (Figure 13), indicated by the discoloration of the dye compared to the UG sample. The G1 samples presented the lowest value for a* parameter. After the thermal shock test, the GW4 samples continued to show photocatalytic activity, while the GW1's photocatalytic activity was diminished but still more efficient than that of the UG sample. Furthermore, the composite performed well in terms of photocatalytic activity on Itaquera granite due to better adhesion to the stone's surface.

All the numeric results of the tests performed for the present study can be found in Table 3.

4. Conclusions

Maintenance and cleaning procedures are essential to the conservation of architectural heritage buildings. Using TiO_2 as a self-cleaning treatment has proven to be a promising way to help with this challenging task.

In our study, we applied a TiO_2-TEOS composite at two different concentrations in two layers by brushing them onto two types of Brazilian stones. This composite presented self-cleaning characteristics and did not alter much the samples' capillarity with 1% TiO_2 (w/v), but also did not adhere to quartz and did not behave as a hydrophobic product.

We observed that the higher the concentration of TiO_2, the greater the self-cleaning properties of the surface; however, a higher concentration also caused greater chromatic changes, resulting in more whitish surfaces and a more hydrophilic character.

The treatment did not present satisfactory results for Itararé sandstone due to its mineralogy, being basically composed of quartz. SEM analyses pointed out that TiO_2 -TEOS did not adhere to quartz and feldspar grains, but

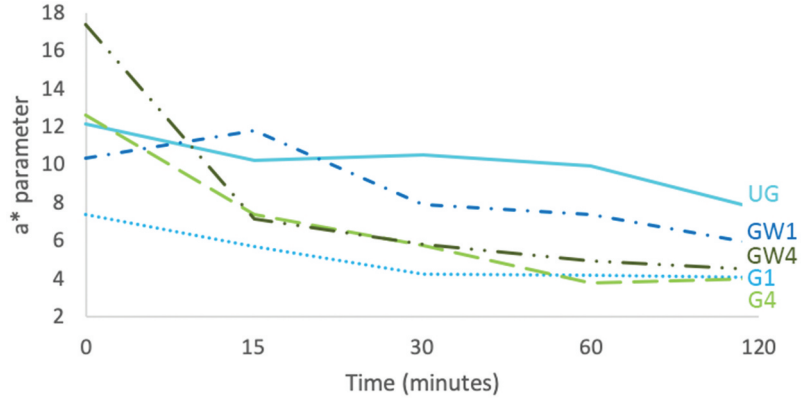

Figure 13. Colour resistance to UV light of Itaquera granite after application of rhodamine B.

in the clay matrix that constitutes only 10–15% of the stone. Due to its porosity, its untreated surface is hydrophilic. With the treatment, the hydrophobicity increases a little, however, after the thermal shock test, this characteristic returns to that presented in the untreated sample. The treatment caused a chromatic variation according to ΔE^* and an increase in the L^* parameter, which whitened the surface of the stone. The photocatalytic activity of TiO_2 was not effective for Itararé sandstone, because there was no more pronounced discoloration of the dye relative to the untreated sample. And finally, the product proved to be ineffective in terms of self-cleaning.

The TiO_2-TEOS composite was efficient in terms of adhesion and photocatalytic activity on Itaquera granite and changed the appearance of the stone to a lesser degree. The lower concentration of TiO_2 showed better colorimetric results, resistance to thermal shock, and self-cleaning properties.

The expected hydrophobicity was not achieved, and further tests will be carried out focusing on this characteristic.

Note from the Authors

This paper is dedicated to the memory of Prof. Valter Ussui who passed away on 21 January 2021. Graduated in Chemistry and PhD in Nuclear Technology, he dedicated most of his careerat IPEN studying chemical processes for ceramic powder synthesis. Part of his contribution to the preservation of architectural heritage is presented in this paper where a titania-silica powders synthesis process was developed.

Acknowledgments

The authors acknowledge the comments and suggestions of the anonymous reviewers, which improved the manuscript.

The authors would like to thank Lucia Shibata for proofreading the article and the members of the CCTM/IPEN Microscopy, XRD, and Cilas laboratories for the technical support they provided.

Disclosure statement

No potential conflict of interest was reported by the author(s).

Funding

This work was supported by the Comissão de Aperfeiçoamento de Pessoal de Nível Superior - CAPES (grant number 88882.315495/201901).

ORCID

Danielle Grossi http://orcid.org/0000-0001-8700-3340
Dolores Ribeiro Ricci Lazar http://orcid.org/0000-0001-7384-304X
Eliane Aparecida Del Lama http://orcid.org/0000-0003-1584-0670
Valter Ussui http://orcid.org/0000-0003-2704-0179

References

Andronic, L., D. Andrasi, A. Enesca, M. Visa, and A. Duta. 2011. The influence of titanium dioxide phase composition on dyes photocatalysis. *Journal of Sol-Gel Science and Technology* 58 (1):201–08. doi:10.1007/s10971-010-2378-3.

Bak, T., L. Wenxian, J. Nowotny, A. J. Atanacio, and J. Davis. 2015. Photocatalytic properties of TiO_2: Evidence of the key role of surface active sites in water oxidation. *The Journal of Physical Chemistry. A* 119 (36):9465–73. doi:10.1021/acs.jpca.5b05031.

Banerjee, S., D. D. Dionysiou, and S. C. Pillai. 2015. Self-cleaning applications of TiO_2 by photo-induced hydrophilicity and photocatalysis. *Applied Catalysis. B, Environmental* :396428. doi:10.1016/j.apcatb.2015.03.058.176177

Berns, R. S. 2000. *Principles of color technology*. 3rd ed. New York: Wiley-Interscience.

Bocardi, L. B., L. A. Fernandes, S. P. Rostirolla, and C. J. Appi. 2006. Diagênese dos Arenitos do Grupo Itararé, Permocarbonífero, Bacia do Paraná. *Revista Brasileira De Geociências* 36 (2):221–31. doi:10.25249/0375-7536.2006362221231.

Carrascosa, L. A. M., D. S. Facio, and M. J. Mosquera. 2016. Producing superhydrophobic coatings for roof tiles. *Nanotechnology* 27 (9):095604. doi:10.1088/0957-4484/27/9/095604.

De Ferri, L., P. P. Lottici, A. Lorenzi, A. Montenero, and G. Vezzalini. 2013. Hybrid sol-gel based coatings for the protection of historical window glass. *Journal Sol-Gel Science Technology* 66 (2):253–63. doi:10.1007/s10971-013-3002-0.

Del Lama, E. A., D. D. L. C. Bacci, L. Martins, M. G. M. Garcia, and L. K. Dehira. 2015. Urban geotourism and the old centre of São Paulo city, Brazil. *Geoheritage* 7 (2):147–64. doi:10.1007/s12371-014-0119-7.

Del Lama, E. A., G. A. J. Szabó, L. K. Dehira, and Y. Kihara. 2008. Impacto do intemperismo no arenito de revestimento do Teatro Municipal de São Paulo. *Geologia USP* 8 (1):75–86. doi:10.5327/Z1519-874X2008000100006.

Del Lama, E. A., L. K. Dehira, and A. C. Reys. 2009. Visão geológica dos monumentos da cidade de São Paulo. *Revista Brasileira De Geociências* 39 (3):409–20. doi:10.25249/0375-7536.2009394409420.

Euvananont, C., C. Junin, K. Inpor, P. Limthongkul, and C. Thanachayanont. 2008. TiO_2 optical coating layers for self-cleaning applications. *Ceramics International* 34 (4):1067–71. doi:10.1016/j.ceramint.2007.09.043.

Feltrin, J., M. N. Sartor, A. De Noni Jr., A. M. Bernardin, D. Hotza, and J. A. Labrincha. 2013. Superfícies fotocatalíticas de titânia em substratos cerâmicos. Parte I: Síntese, estrutura e fotoatividade [Photocatalytic surfaces of titania on ceramic substrates. Part I: Synthesis, structure and photoactivity]. *Cerâmica* 59 (352):620–32. doi:10.1590/S0366-69132013000400020.

Fiorentino, S., G. C. Grillini, and M. Vandini. 2015. The national monument to Francesco Baracca in Lugo di Romagna (Ravenna, Italy): Materials, techniques and conservation aspects. *Case Studies in Construction Materials* 3:19–32. doi:10.1016/j.cscm.2015.05.003.

Flores-Colen, I., A. Soares, and J. Brito. 2013. A natotecnologia aplicada às argamassas de revestimento. *Revista Internacional* 34 (11):42–51.

Fort, R., M. J. Varas, M. Alvarez de Buergo, and D. Martin-Freire. 2011. Determination of anisotropy to enhance the durability of natural Stone. *Journal of Geophysics and Engineering* 8 (3):S132–S144. doi:10.1088/1742-2132/8/3/S13.

Franzoni, E., A. Fregni, R. Gabrielli, G. Graziani, and E. Sassoni. 2014. Compatibility of photocatalytic TiO_2 -based finishing for renders in architectural restoration: A preliminary study. *Building and Environment* 80:125–35. doi:10.1016/j.buildenv.2014.05.027.

Freire-Lista, D. M., and R. Fort. 2017. Exfoliation microcracks in building granite. Implications for anisotropy. *Engineering Geology* 220:85–93. doi:10.1016/j.enggeo.2017.01.027.

Fujishima, A., T. N. Rao, and D. A. Tryk. 2000. Titanium dioxide photocatalysis. *Journal of Photochemistry and Photobiology C: Photochemistry Reviews* 1 (1):1–21. doi:10.1016/S1389-5567(00)00002-2.

Gherardi, F., A. Colombo, M. D'Arienzo, B. Di Credico, S. Goidanich, F. Morazzoni, R. Simonutti, and L. Toniolo. 2016. Efficient self-cleaning treatments for built heritage based on highly photo-active and well dispersible TiO_2 nanocrystals. *Microchemical Journal* 126:54–62. doi:10.1016/j.microc.2015.11.043.

Gherardi, F., S. Goidanish, and L. Toniolo. 2018. Improvements in marble protection by means of innovative photocatalytic nanocomposites. *Progress in Organic Coatings* 121:13–22. doi:10.1016/j.porgcoat.2018.04.010.

Gimenez, A. M. S. 2018. Suscetibilidade experimental de rochas do patrimônio histórico aos agentes do intemperismo. PhD thesis, Instituto de Geociências, Universidade de São Paulo. doi: 10.11606/T.44.2018.tde-10072018-152157.

Goffredo, G. B., S. Accoroni, C. Totti, T. Romagnoli, L. Valentini, and P. Munafò. 2017. Titanium dioxide based nanotreatment to inhibit microalgal fouling on building stone surfaces. *Building and Environment* 112:209–22. doi:10.1016/j.buildenv.2016.11.034.

Graziani, L., E. Quagliarini, A. Osimani, L. Aquilanti, F. Clementi, C. Yéprémian, V. Laricca, S. Amoroso, and M. D'Orazio. 2013. Evaluation of inhibitory effect of TiO_2 nanocoatings against microalgal growth on clay brick façades under weak UV exposure conditions. *Building and Environment* 64:38–45. doi:10.1016/j.buildenv.2013.03.003.

Graziani, L., E. Quagliarini, and M. D'Orazio. 2016. The role of roughness and porosity on the self-cleaning and anti-biofouling efficiency of TiO_2-Cu and TiO_2-Ag nanocoatings applied on fired bricks. *Construction and Building Materials* 129:116–24. doi:10.1016/j.conbuildmat.2016.10.111.

Grossi, D. 2016. Avaliação da aplicação de consolidantes no Arenito Itararé, constituinte da fachada do Teatro Municipal de São Paulo. PhD thesis, Instituto de Geociências, Universidade de São Paulo. doi: 10.11606/T.44.2018.tde-28062018-085428.

Grossi, D., and E. A. Del Lama. 2018. Avaliação da eficácia de hidrofugantes e antigraffiti no Arenito Itararé. *Geologia USP* 18 (4):43–55. doi:10.11606/.2316-9095.v18-144298.

Hanaor, D. A. H., and C. C. Sorrell. 2011. Review of the anatase to rutile phase transformation. *Journal of Materials Science* 46 (4):855–74. doi:10.1007/s10853-010-5113-0.

Hendrix, Y., A. Lazaro, Q. L. Yu, and H. J. H. Brouwers. 2019. Influence of synthesis conditions on the properties of photocatalytic titania-silica composites. *Chemistry* 371:25–32. doi:10.1016/j.jphotochem.2018.10.040.

Hilonga, A., J. K. Kim, P. B. Sarawade, and H. T. Kim. 2010. Mesoporous titania–silica composite from sodium silicate and titanium oxychloride. Part I: Grafting method. *Journal of Materials Science* 45 (5):1255–63. doi:10.1007/s10853-009-4076-5.

Kaleji, B. K., R. Sarraf-Mamoory, K. Nakata, and A. Fujishima. 2011. The effect of Sn dopant on crystal structure and photocatalytic behavior of nanostructured titania thin films. *Journal of Sol-Gel Science and Technology* 60 (2):1–9. doi:10.1007/s10971-011-2560-2.

Kapridaki, C., and P. Maravelaki-Kalaitzaki. 2013. TiO_2–SiO_2–PDMS nano-composite hydrophobic coating with self-cleaning properties for marble protection. *Progress in Organic Coatings* 76 (23):40010. doi:10.1016/j.porgcoat.2012.10.006.

La Russa, M. F., A. Macchia, S. A. Ruffolo, F. De Leo, M. Barberio, P. Barone, G. M. Crisci, and C. Urzì. 2014. Testing the antibacterial activity of dopped TiO_2 for preventing biodeterioration of cultural heritage building materials. *International Biodeterioration & Biodegradation* 96:87–96. doi:10.1016/j.ibiod.2014.10.002.

La Russa, M. F., S. A. Ruffolo, N. Rovella, C. M. Belfiore, A. M. Palermo, M. T. Guzzi, and G. M. Crisci. 2012. Multifunctional TiO_2 coatings for cultural heritage. *Progress in Organic Coatings* 74 (1):186–91. doi:10.1016/j.porgcoat.2011.12.008.

Maravelaki-Kalaitzaki, P., N. Kallithrakas-Kontos, Z. Agioutantis, S. Maurigiannakis, and D. Korakaki. 2008. A comparative study of porous limestones treated with silicon-based strengthening agents. *Progress in Organic Coatings* 62 (1):49–60. doi:10.1016/j.porgcoat.2007.09.020.

Morenghi, C. L. 2007. Arcabouço estratigráfico e potencial de armazenamento em arenitos permocarboníferos do Grupo Itararé na região do Alto Estrutural de Pitanga, centro-leste do Estado de São Paulo. Master dissertation, Instituto de Geociências, Universidade de São Paulo.

Mosquera, M. J., D. M. de los Santos, L. Valdez-Castro, and L. Esquivias. 2008. New route for producing crack-free xerogels: Obtaining uniform pore size. *Journal of Non-Crystalline Solids* 354 (29):64550. doi:10.1016/j.jnoncrysol.2007.07.095.

Munafó, P., G. B. Goffredo, and E. Quagliarini. 2015. TiO2-based nanocoatings for preserving architectural stone surfaces: An overview. *Construction and Building Materials* 84:201–18. doi:10.1016/j.conbuildmat.2015.02.083.

Nakajima, A., S.-I. Koizumi, T. Watanabe, and K. Hashimoto. 2000. Photoinduced amphiphilic surface on polycrystalline anatase TiO_2 thin films. *Langmuir* 16 (17):7048–50. doi:10.1021/la0004348.

Neves, L. E. B. 1968. Estudo prático de argilas por difratometria de raios-X. *Boletim Técnico PETROBRÁS* 11 (1):123–35.

Nogueira, R. F. P., and W. F. Jardim. 1998. A fotocatálise heterogênea e sua aplicação ambiental [Heterogeneous photocatalysis and its environmental applications]. *Química Nova* 21 (1):69–72. doi:10.1590/S0100-40421998000100011.

Ortiz, P., V. Antúnez, R. Ortiz, J. M. Martín, M. A. Gómez, A. R. Hortal, and B. Martínez-Haya. 2013. Comparative study of pulsed laser cleaning applied to weathered marble surfaces. *Applied Surface Science* 283:193–201. doi:10.1016/j.apsusc.2013.06.081.

Pedna, A., L. Pinho, P. Frediani, and M. J. Mosquera. 2016. Obtaining SiO_2–fluorinated PLA bionanocomposites with application as reversible and highly-hydrophobic coatings of buildings. *Progress in Organic Coatings* 90:91–100. doi:10.1016/j.porgcoat.2015.09.024.

Pénard, A., T. Gacoin, and J. Boilot. 2007. Functionalized sol–gel coatings for optical applications. *Accounts of Chemical Research* 40 (9):895–902. doi:10.1021/ar600025j.

Pinho, L., and M. J. Mosquera. 2011. Titania-silica nanocomposite photocatalysts with Application in stone self-cleaning. *Journal of Physical Chemistry C* 115 (46):22851–62. doi:10.1021/jp2074623.

Pinho, L., and M. J. Mosquera. 2013. Photocatalytic activity of TiO_2–SiO_2 nanocomposites applied to buildings: Influence of particle size and loading. *Applied Catalysis. B, Environmental* 134135:20521. doi:10.1016/j.apcatb.2013.01.021.

Pohl, M. C. 1998. Light scattering. In *ASM handbook*, ed. P. K. Samal, and J. W. Newkirk, Vol. 7, 1st ed., 250–55. Ohio: Metals Park.

Poulios, I., P. Spathis, A. Grigoriadou, K. Delidou, and P. Tsoumparis. 1999. Protection of marbles against corrosion and microbial corrosion with TiO_2 coatings. *Journal of Environment Science and Health, Part A: Environmental Science* 34 (7):1455–71. doi:10.1080/10934529909376905.

Price, C. A. 2006. Consolidation. In *Stone conservation: Principles and practice*, ed. A. Henry, 101–25. United Kingdon: Donhead.

Quagliarini, E., F. Bondioli, G. B. Goffredo, A. Lucciulli, and P. Munafò. 2012. Smart surfaces for architectural heritage: Preliminary results about the application of TiO_2-based coatings on travertine. *Journal of Cultural Heritage* 13 (2):204–09. doi:10.1016/j.culher.2011.10.002.

Quagliarini, E., F. Bondioli, G. B. Goffredo, A. Lucciulli, and P. Munafò. 2013. Self-cleaning materials on architectural heritage: Compatibility of photo-induced hydrophilicity of TiO_2 coatings on stone surfaces. *Journal of Cultural Heritage* 14 (1):1–7. doi:10.1016/j.culher.2012.02.006.

Rao, K. V. S., M. Subrahmanyam, and P. Boule. 2004. Immobilized TiO_2 photocatalyst during long-term use: Decrease of its activity. *Applied Catalysis. B, Environmental* 49 (4):239–49. doi:10.1016/j.apcatb.2003.12.017.

Reghunath, S., D. Pinheiro, and K. R. S. Devi. 2021. A review of hierarchical nanostructures of TiO_2. *Advances and Applications. Applied Surface Science Advances* 3:100063. doi:10.1016/j.apsadv.2021.100063.

Ruot, B., A. Plassais, F. Olive, L. Guillot, and L. Bonafous. 2009. TiO_2-containing cement pastes and mortars: Measurements of the photocatalytic efficiency using a rhodamine B-based colourimetric test. *Solar Energy* 83 (10):1794–801. doi:10.1016/j.solener.2009.05.017.

Sasse, H. S., and R. Snethlage. 1996. Methods for the evaluation of stone conservation treatments. In *Dahlem workshop on saving our architectural heritage*, ed. H. S. Sasse, and R. Snethlage, 223–43. Berlin: John Willey & Sons.

Scharnberg, A. R. A., A. C. Loreto, T. B. Wermuth, A. K. Alves, S. Arcaro, P. A. M. Santos, and A. A. L. Rodriguez. 2020. Porous ceramic supported TiO_2 nanoparticles: Enhanced photocatalytic activity for Rhodamine B degradation. *Boletín De La Sociedad Española De Cerámica Y Vidrio* 59 (6):230–38. doi:10.1016/j.bsecv.2019.12.001.

Sena da Fonseca, B., A. P. F. Pinto, S. Piçarra, and M. F. Montemor. 2017. Artificial aging route for assessing the potential efficacy of consolidation treatments applied to porous carbonate stones. *Materials & Design* 120:10–21. doi:10.1016/j.matdes.2017.02.001.

Shtyka, O., V. Shatsila, R. Ciesielski, A. Kedziora, W. Maniukiewicz, S. Dubkov, D. Gromov, A. Tarasov, J. Rogowski, A. Stadnichenko, et al. 2021. Adsorption and photocatalytic reduction of Carbon Dioxide on TiO_2. *Catalysts* 11 (1):47. doi:10.3390/catal11010047.

Sikora, P., K. Cendrowski, A. Markowska-Szczupak, E. Horszczaruk, and E. Mijowska. 2017. The effects of silica/titania nanocomposite on the mechanical andbactericidal properties of cement mortars. *Construction and Building Materials* 150:738–46. doi:10.1016/j.conbuildmat.2017.06.054.

Snethlage, R., and K. Sterflinger. 2011. Stone conservation. In *Stone in architecture*, ed. S. Sigesmund, and R. Snethlage, 411–34. Londres: Springer.

Sun, A. H., P. J. Guo, Z. X. Li, Y. Li, and P. Cui. 2009. Low temperature synthesis of anatase and rutile titania nanopowders by hydrolysis of $TiCl_4$ using ammonia gas. *Journal of Alloys and Compounds* 481 (12):60509. doi:10.1016/j.jallcom.2009.03.045.

Toreno, G., D. Isola, P. Meloni, G. Carcangiu, L. Selbmann, S. Onofri, and L. Zucconi. 2018. Biological colonization on stone monuments: A new low impact cleaning method. *Journal of Cultural Heritage* 30:100–09. doi:10.1016/j.culher.2017.09.004.

Ussui, V., F. Leitão, C. Yamagata, C. A. B. Menezes, D. R. R. Lazar, and J. O. A. Paschoal. 2003. Synthesis of ZrO_2-based ceramics for application in SOFC. *Materials Science Forum* 416418:68187. 10.4028/www.scientific.net/MSF.416-418.681.

Vieira, L. A. 2016. Nanomateriais aplicados ao patrimônio cultural amazônico: Revestimentos autolimpantes de dióxido de titânio em calcário Lioz. Master dissertation. Universidade Federal do Pará.

Wheeler, G. 2005. *Alkoxisilanes and the consolidation of stone*. 1st ed. Los Angeles: Getty Institute.

Windler, L., C. Lorenz, N. Von Goetz, K. Hungerbühler, M. Amberg, M. Heuberger, and B. Nowack. 2012. Release of titanium dioxide from textiles during washing. *Environmental Science & Technology* 46 (15):8181–88. doi:10.1021/es301633b.

Xu, F., L. Dan, Q. Zhang, H. Zhang, and J. Xu. 2012. Effects of addition of coloidal silica particles on TEOS-based stone protection using n-octylamineas a catalyst. *Progress in Organic Coatings* 75 (4):429–34. doi:10.1016/j.porgcoat.2012.07.00.

Zanfir, A. V., G. Voicu, A. I. Bădănoiu, D. Gogan, O. Oprea, and E. Vasile. 2018. Synthesis and characterization of titania-silica fume composites and their influence on the strength of self-cleaning mortar. *Composites Part B: Engineering* 140:157–63. doi:10.1016/j.compositesb.2017.12.032.